THE JOURNAL OF PHYSICAL CHEMISTRY A

Article

pubs.acs.org/JPCA

Enhancing Excited State Intramolecular Proton Transfer in 2-(2′-Hydroxyphenyl)benzimidazole and Its Nitrogen-Substituted Analogues by β-Cyclodextrin: The Effect of Nitrogen Substitution#

Francis A. S. Chipem, Santosh Kumar Behera, and G. Krishnamoorthy*

Department of Chemistry, Indian Institute of Technology Guwahati, Guwahati 781 039, Assam, India

Supporting Information

ABSTRACT: Excited state intramolecular proton transfer (ESIPT) in nitrogen-substituted analogues of 2-(2′-hydroxyphenyl)benzimidazole (HPBI), 2-(2′-hydroxyphenyl)-3*H*-imidazo[4,5-*b*]pyridine (HPIP-b), and 2-(2′-hydroxyphenyl)-3*H*-imidazo-[4,5-*c*]pyridine (HPIP-c) have been investigated in a β-cyclodextrin (β-CD) nanocavity and compared with that of HPBI. The stoichiometry and the binding constants of the complexes were determined by tautomer emissions. Both pK_a and NMR experiments were employed to determine the orientation of the molecules inside of the β-CD cavity. Huge enhancement in the tautomer emission of HPIP-b and HPIP-c compared to that of HPBI in β-CD suggests that not only is the ESIPT favored inside of the cavity, but also, the environment reduces the nonradiative decay through the formation of an intramolecular charge-transfer (ICT) state. Unlike HPBI, the tautomer emission to normal emission ratio of HPIP-b increases from 0.9 to 2.6, and that of HPIP-c increases from 4.9 to 7.4 in 15 mM β-CD. The effect of dimethylsulfoxide (DMSO) on complexation was also investigated for all three guest molecules. In DMSO, HPBI is present in neutral form, but the nitrogen-substituted analogues are present in both neutral and monoanionic forms. However, in DMSO upon encapsulation by β-CD, all three molecules are present in both neutral and monoanionic forms in the nanocavity. The monoanion is stabilized more inside of the β-CD cavity. The studies revealed that the ESIPT of nitrogen-substituted analogues is more susceptible to the environment than HPBI, and therefore, they are more promising probes.

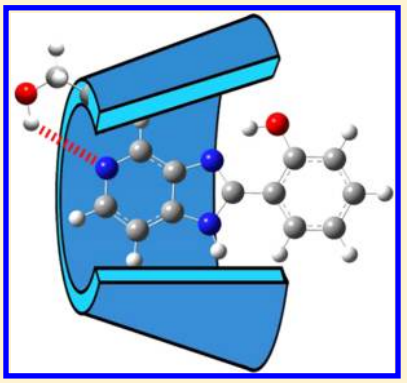

1. INTRODUCTION

Studies on organized microheterogeneous assemblies have been growing rapidly during the past few decades as these serve as good miniature models for studying and mimicking important phenomena in biosystems.[1−3] Among the studies on microheterogeneous media, inclusion complexes are one of the interesting subjects for many researchers. Inclusion complexes provide valuable information about noncovalent intermolecular interactions between the host and guest molecules where the guest component is lying within the cavity of the host molecule without forming any covalent bond.[1] Apart from biomimicking,[2,4] inclusion complexes find applications in drug delivery,[3] nanosized electronic devices,[5] and energy storage devices.[6]

Cyclodextrins (CDs)[1−3,5] are the most sought systems for studying such inclusion complexes. CDs are cyclic oligosaccharides composed of glucopyranose units linked by α-(1,4) bonds with hydrophilic external walls and an interior hydrophobic nanosized cavity of different size and shape.[1−3] The hydrophobicity of the cavity enhances the solubility[7] and the fluorescence of the encapsulated guest molecule.[8] Therefore, CDs have been used as microenvironments to study excited-state processes such as proton transfer,[8−10] charge transfer,[11−13] and energy transfer.[14,15] Douhal et al. reviewed the dynamics and structural aspects of the host−guest interaction in CD.[16,17] The inclusion complexes of fluorophore in aqueous host molecules including CDs were recently reviewed by Nau et al.[18] Wagner more recently reviewed the hydrogen bonding of excited states in supramolecular inclusion complexes including CDs.[19]

Douhal et al. investigated the effect of β-CD on the dynamics of an excited-state intramolecular proton transfer (ESIPT) molecule.[16] Warner et al. studied the dual fluorescence of 10-hydroxybenzo[*h*]quinone and also 2-(2′-hydroxyphenyl)-benzimidazole (HPBI), its corresponding benzoxazole, and benzothiazole in the presence of β-CD.[20,21] They showed the existence of weak intramolecular hydrogen bonding in HPBI and formation of strong intermolecular hydrogen bonds with the hydroxyl groups of CD. They further showed that the phototautomers exist as zwitterions. More recently, Guchhait et al. studied the ESIPT process of 1-hydroxy-2-napthaldehyde in CDs.[22]

HPBI and its analogues form a class of fluorophores that are extensively studied due to the ESIPT exhibited by them.[21,23−40] Hence, this class of compounds finds applications as lasers, probes, sensors, and devices.[25,34,41−43] The ESIPT reaction is greatly affected by the hydrogen bonding capability of the solvent.[44−49] In protic solvents, the intramolecular hydrogen bonded ring in the fluorophore molecule might break to form

Received: November 19, 2012
Revised: April 26, 2013
Published: April 26, 2013

an intermolecular hydrogen bond between the fluorophore and the solvent molecules. This reduces the formation of the phototautomer, which decreases the tautomer emission and increases the normal emission. However, in aprotic solvents, the tautomer emission is predominant, and the normal emission is weak. In addition, at different pHs, these molecules exist in different forms, namely, neutrals, anions, cations, zwitterions, and tautomers, giving different emissions.

Despite the fact that the utility of HPBI as a fluorescent probe was well-established,[22,23,50,51] the utility of its nitrogen analogues 2-(2′-hydroxyphenyl)-3*H*-imidazo[4,5-*b*]pyridine (HPIP-b) and 2-(2′-hydroxyphenyl)-3*H*-imidazo[4,5-*c*]-pyridine (HPIP-c) are not investigated. Chattopadhyay pointed out that although the ESIPT process is affected by the microheterogeneous media, it also strongly depends on the nature of the molecule.[52] Interestingly, substitution of the N-heteroatom in the benzene ring of HPBI reduces the quantum yield,[35−37,53,54] and on the other hand, nitrogen substitution on the phenolic ring increases the quantum yield.[54−56] Theoretical calculations predicted that the proton-coupled charge-transfer state may act as the major nonradiative decay channel for the proton-transferred tautomer.[34,53−59] The ESIPT is accompanied by a torsion rotation of the two aromatic rings, which leads to an intramolecular charge transfer (ICT) state from where the nonradiative decay occurs. This should increase environmental sensitivity of the nitrogen-substituted analogues more than that of HPBI. Therefore, we also explore the efficiency of these fluorophores as potential fluorescence probes by investigating the properties of these molecules in CD utilizing the ESIPT reaction. β-CD is the most common CD, and it has a sufficient diameter to encapsulate a variety of aromatic guest molecules firmly and tightly, while other CDs have a too small or too large cavity to make strong binding.[18,60] It can also accommodate HPBI and its analogues lengthwise without hindrances. HPBI is already studied in β-CD,[21] and phenylimidazopyridine derivatives, structurally related molecules of HPBI, also have a higher binding affinity for β-CD.[11,61] Therefore, we have chosen the β-CD nanocavity for the present studies.

2. MATERIALS AND METHODS

HPBI, HPIP-b, and HPIP-c were synthesized by the condensation of salicylic acid with *ortho*-phenylenediamine, 2,3-diaminopyridine, and 3,4-diaminopyridine, respectively, in polyphosphoric acid by following the method described elsewhere.[25,35,37] The compounds were recrystallized four times in methanol before use. β-CD from Sigma Aldrich and HPLC-grade dimethylsulfoxide (DMSO) from Merck India were used as received. Millipore water was used for preparing aqueous solution. The pH of the solutions was adjusted by addition of small amount of sodium hydroxide and sulfuric acid solution.

HPBI: ^{1}H NMR (400 MHz, DMSO-d_6) δ 7.01 (1H, d, Ar−H), 7.05 (1H, d, Ar−H), 7.28 (2H, br, Ar−H), 7.38 (1H, m, Ar−H), 7.61 (1H, br, Ar−H), 7.70 (1H, br, Ar−H), 8.02 (1H, d, ArN-H). ^{13}C NMR (300 MHz, DMSO-d_6) δ 112.74, 117.38, 118.17, 119.39, 122.67, 123.52, 126.36, 131.99, 151.83, 158.11. IR (KBr pellets): 3325, 3056, 2508, 1602, 1590, 1492, 1395, 1262, 726 cm^{-1}.

HPIP-b: ^{1}H NMR (400 MHz, DMSO-d_6) δ 7.02 (2H, d, Ar−H), 7.30 (1H, m, Ar−H), 7.42 (1H, t, Ar−H), 8.04 (1H, d, Ar−H), 8.11 (1H, d, Ar−H), 8.39 (1H, d, Ar−H). ^{13}C NMR (300 MHz, DMSO-d_6) δ 112.39, 116.05, 117.63, 119.01, 119.69, 127.02, 128.86, 132.84, 144.67, 153.50, 158.47. IR (KBr pellets): 3432, 3064, 1634, 1588, 1491, 1422, 1259, 740 cm^{-1}.

HPIP-c: ^{1}H NMR (400 MHz, DMSO-d_6) δ 6.98 (1H, d, Ar−H), 7.04 (1H, d, Ar−H), 7.39 (1H, t, Ar−H), 7.69 (1H, d, Ar−H), 8.11 (1H, d, Ar−H), 8.28 (1H, d, Ar−H), 8.94 (1H, s, Ar−H). ^{13}C NMR (300 MHz, DMSO-d_6) δ 109.85, 113.63, 117.38, 119.57, 127.64, 132.57, 136.89, 137.77, 139.50, 156.95, 158.27. IR (KBr pellets): 3505, 3044, 1632, 1590, 1491, 1415, 1288, 1259, 754 cm^{-1}.

The absorbance and steady-state fluorescence spectra were recorded with a Cary 100 spectrophotometer and Horiba Jobin Yvon Fluoromax 4 fluorimeter, respectively. The excitation and emission slit widths for fluorescence measurements were 1 nm. Quantum yields were measured using quinine sulfate in 1 N sulfuric acid (Φ_f = 0.546)[62] as the standard. Lifetime measurements were performed on a time-correlated single-photon counting (TCSPC)-based Edinburgh instrument Life-Spec II using PicoQuant's 308 nm LED and Edinburgh instrument's 375 nm laser diode as light sources with full pulse widths of 635 and 2 ps, respectively, at half-maximum. The emission slit widths used in the lifetime measurements were 20 nm in the case of the 308 nm LED and 10 nm in the case of the 375 nm laser diode. The concentrations of the fluorophores were 5 μM in all of the absorption and fluorescence spectral measurements performed for the neutral form of the fluorophores. The concentrations were 10 μM for spectral measurements of monocationic forms. ^{1}H NMR spectra were obtained from a 400 MHz NMR spectrometer and ^{13}C NMR spectra were obtained from a 300 MHz NMR spectrometer. All of the experiments were performed at room temperature (298 ± 3 K).

3. RESULTS AND DISCUSSION

3.1. Absorption Spectra. HPIP-b and HPIP-c have low solubility in water, but their solubility enhances in the presence of β-CD. This enhancement in solubility is an indication of inclusion complex formation by the encapsulation of the fluorophores in the hydrophobic cavity of β-CD. The effects of β-CD on the absorption spectra of HPIP-b and HPIP-c in water are depicted in Figure 1. Though absorbance maxima of both HPIP-b and HPIP-c are nearly unaffected with the increase in concentration of β-CD, a small hyperchromic effect is observed. These increases in absorbance are attributed to the detergent action of the host molecule β-CD on the guest molecule, which also confirms the formation of the host−guest inclusion complex.[63,64]

The effects of β-CD on the absorption spectra of HPBI and its analogues in DMSO are presented in Figure 2. The same as in aqueous solution, with the addition of β-CD, there is hyperchromic effect in the absorption spectra of HPBI and HPIP-c (Figure 2a and c). The changes in absorption spectra of HPIP-b in DMSO are different in the sense that isosbestic points are observed (Figure 2b). However, the most striking difference between DMSO and aqueous solution is the appearance of a weak new band at around 365 nm in HPIP-b and HPIP-c. The band's absorption is very little in DMSO but increases with an increase in concentration of β-CD in DMSO. In HPBI though, the red-shifted band is absent in the absence of β-CD in DMSO; it appears in DMSO at higher concentrations of β-CD.

3.2. Fluorescence Emission Spectra. In aqueous solution upon excitation at 310 nm, HPIP-b exhibits both normal and tautomer emissions (Figure 3a). A small enhancement is

dx.doi.org/10.1021/jp311438s | J. Phys. Chem. A 2013, 117, 4084−4095

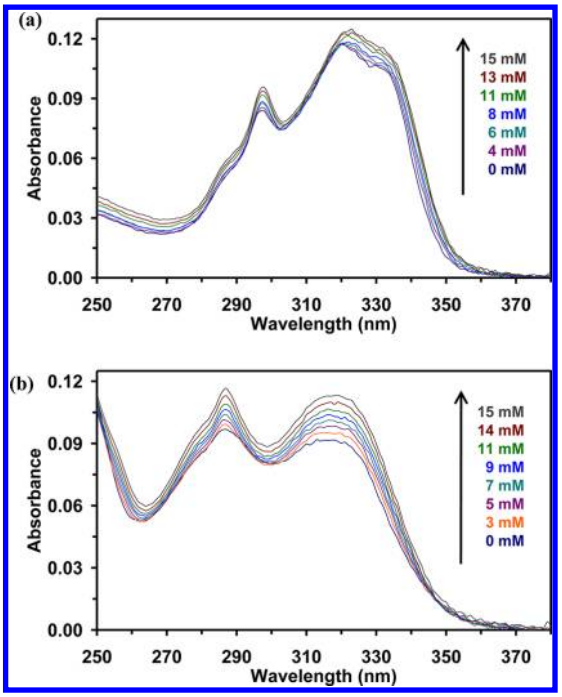

Figure 1. Absorption spectra of (a) HPIP-b and (b) HPIP-c at different concentrations of β-CD in water.

observed in the intensity of the normal emission. However, there is a significant change in the tautomer fluorescence of HPIP-b in aqueous solution with increasing β-CD concentration. While the emission maximum of the normal band at 365 nm is nearly unaffected, that of the tautomer band is red-shifted by 16 nm from 468 nm in an aqueous medium to 484 nm with 15 mM β-CD, with substantial enhancement in fluorescence. While the full width at half-maximum (fwhm) of the normal band is 4610 cm^{-1} in the absence of β-CD, that in the presence of β-CD is 4155 cm^{-1}. The fwhm of the tautomer band decreases from 5635 cm^{-1} in the absence of β-CD to 3170 cm^{-1} with 15 mM β-CD. The quantum yield ratio of the tautomer to normal emission (Φ_T/Φ_N) increases from 0.9 (in the absence of β-CD) to 2.6 (at a 15 mM concentration of β-CD; Figure 4). The effects of β-CD on fluorescence characteristics of HPIP-c in aqueous media are a little different from that of HPIP-b (Figure 3b). The intensity of the normal emission is reduced with an increase in tautomer emission with a quasi-isoemissive point. The presence of a quasi-isoemissive point is due to the existence of a *cis*-enol/*trans*-enol equilibrium. However, a clear isoemissive point is not observed, owing to the increase in the radiative decay of *trans*-enol inside of the CD cavity. In HPIP-b, the enhancement in radiative decay of *trans*-enol upon encapsulation dominates over the decrease in the population of *trans*-enol. Therefore, even the quasi-isoemissive point is not observed (Figure 3a).

Compared to that of HPIP-b, the increase in tautomer emission of HPIP-c is relatively smaller in magnitude. The tautomer band is red-shifted from 464 nm at 0 mM to 469 nm at 15 mM β-CD. The fwhm of the tautomer band decreases from 3715 cm^{-1} in the absence of β-CD to 3400 cm^{-1} with 15 mM β-CD. The Φ_T/Φ_N ratio increases from 4.9 at 0 mM β-CD to 7.4 at a 15 mM concentration of β-CD (Figure 4). The value of the effective dielectric constant of the environment was calculated using a dioxane–water mixture.[65] From the plot of the tautomer emission maxima in a dioxane–water mixture

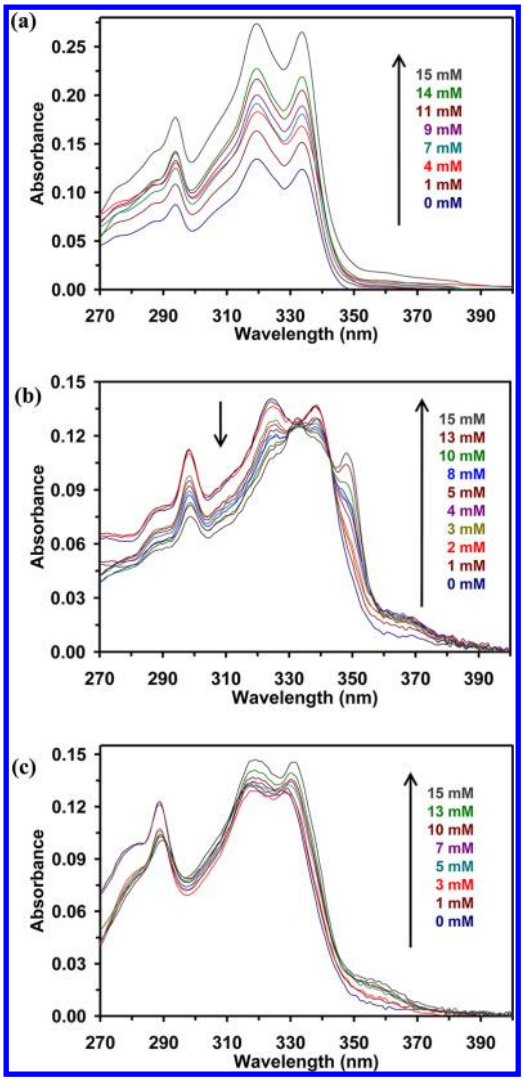

Figure 2. Absorption spectra of (a) HPBI, (b) HPIP-b, and (c) HPIP-c in increasing concentrations of β-CD in DMSO.

versus the dielectric constant of the dioxane–water mixture (Supporting Information Figure S10), the dielectric constant of the environment is estimated to be 37 and 34, respectively, for HPIP-b and HPIP-c. The estimated polarity is in reasonable agreement with the literature reports that the estimated polarity of β-CD is similar to that of the methanol–water mixture.[11,66]

Red shifts are observed in the tautomer bands of HPIP-b and HPIP-c upon decreasing the polarity of the environment.[35,36] Therefore, the red shift suggests the inclusion of the guest molecule into the hydrophobic cavity of the host β-CD. This is further substantiated by the decrease in the fwhm of the tautomer band due to reduction in solvated structures. The enhancement of tautomer emission in the β-CD complex can be explained as follows. HPBI and its analogues are present in both *cis*- and *trans*-enol forms.[30,35,36,53] *cis*-Enol is less polar than *trans*-enol.[53] The closed *cis*-enol upon excitation exclusively undergoes ESIPT to form a tautomer, and the *trans*-enol upon excitation gives normal emission. Protic solvent breaks the intramolecular hydrogen bond and forms more solvated *trans*-enol that lead to an increase in normal emission. In HPBI and its nitrogen-substituted analogues, the decreases in polarity of the environment shifts the *cis*-enol/*trans*-enol equilibrium toward *cis*-enol.[25,35,37] This is evident from the

dx.doi.org/10.1021/jp311438s | J. Phys. Chem. A 2013, 117, 4084–4095

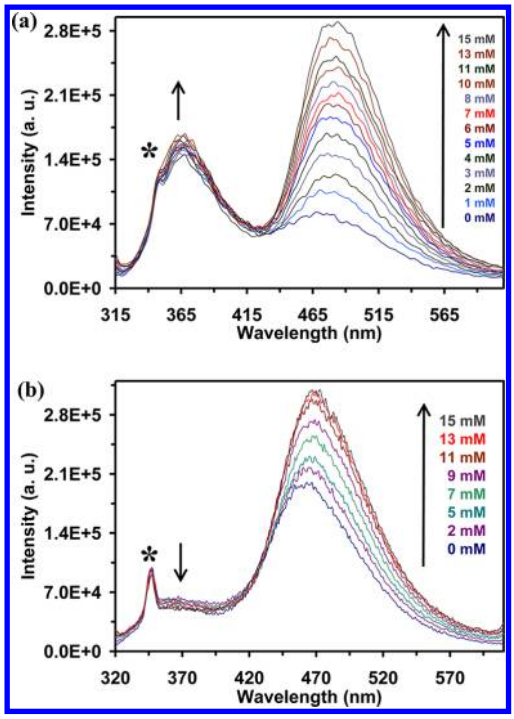

Figure 3. Fluorescence spectra of (a) HPIP-b and (b) HPIP-c at different concentrations of β-CD in water (λ_{exc} = 310 nm). (* denotes water Raman)

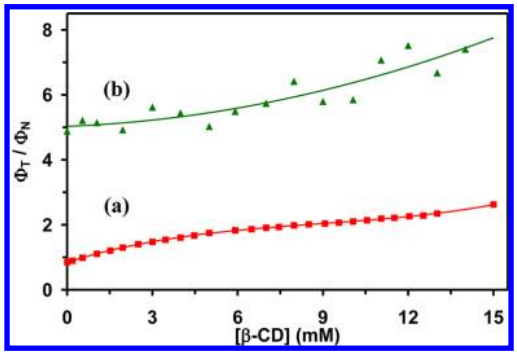

Figure 4. Plot of the quantum yield ratio of the tautomer to normal band of (a) HPIP-b and (b) HPIP-c against [β-CD] in water (λ_{exc} = 310 nm).

increases in the tautomer to normal band ratios with the decrease in polarity of the environment. Therefore, upon encapsulation, the decrease in polarity should shift the equilibrium toward *cis*-enol, and the increase in the relative population of *cis*-enol would result in the enhancement of the tautomer emission. However, an increase in the relative population of *cis*-enol is not the sole factor that leads to an increase in the tautomer emission. The other factor that is responsible for the increase in the tautomer fluorescence is the decrease in the nonradiative decay in the inclusion complex. It should be noted here that torsional-induced rotational relaxation of the phototautomer to nonemissive ICT acts as a nonradiative channel for the deactivation of the excited tautomer.[53,57−59] At twisted geometry, the energy is minimum in the excited state and maximum in the ground state.[53] Thus, the energy gap is less, which favors the nonradiative deactivation. Rodríguez et al. found that the radiationless deactivation channel was enhanced in HPIP-b both upon deprotonation of the hydroxyl group and protonation of the pyridine nitrogen.[67] The deprotonation of hydroxyl group is supposed to increase the charge on the donor, and the proton of the pyridine nitrogen enhances the electron-withdrawing ability of the acceptor, and therefore, they also attributed the nonradiative decay to formation of a nonfluorescent ICT state.[67] In a related study, Rodríguez et al. also reported that when the electron-withdrawing ability of the imidazopydrine ring of HPIP-b is increased by methylation at the pydridine nitrogen, it becomes nonfluorescent due to ESIPT followed by torsional relaxation to the ICT state.[39] More recently, Sekiya et al. detected the twisted conformers of HPBI, those formed through torsional rotation of the excited tautomer in polymorphs of HPBI.[68] Douhal et al. also reported that the twisting motion of 2-(2′-hydroxyphenyl)-4-methyloxazole after ESIPT is restricted by the β-CD nanocavity.[69]

Warner et al. reported that the fluorescence spectrum of HPBI in aqueous β-CD remains unaffected except for small red shift in the longer-wavelength emission.[21] However, unlike HPBI, significant changes are observed in the tautomer emission of nitrogen-substituted analogues upon encapsulation in an aqueous β-CD cavity. The tremendous increase is also observed in the tautomer to normal emission ratio. All of these suggest that the nitrogen substitution makes HPIP-b and HPIP-c sensitive to the environment and can be a better ratiometric probe than HPBI. Our earlier theoretical studies on HPBI and its analogues suggested that nitrogen substitution increases the torsional-induced formation of a nonemissive ICT state.[53] This is due to the higher electron-accepting capability of the imidazopyridyl moiety over the benzimidazolyl moiety. In addition, hydrogen bonding of the solvent with pyridine nitrogen increases the electron-withdrawing ability of the

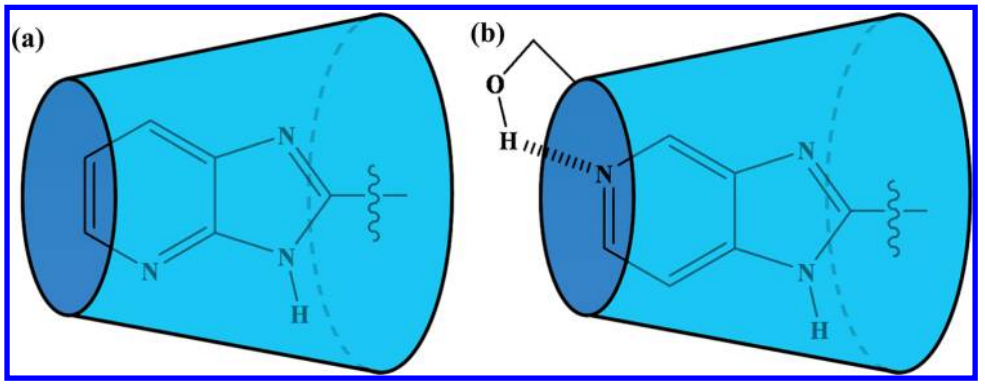

Figure 5. Sites of hydrogen bond formation with the imidazopyridyl moiety of (a) HPIP-b and (b) HPIP-c in a β-CD nanocavity.

dx.doi.org/10.1021/jp311438s | J. Phys. Chem. A 2013, 117, 4084−4095

imidazopyridine ring that increases ICT. In 2-(4′-*N*,*N*-dimethylaminophenyl)imidazopyridines also, it is reported that the hydrogen bonding of the solvent with pyridine nitrogen induces the ICT.[70−72] Rodríguez et al. found that the pyridine nitrogen methylated derivative of HPIP-b is non-fluorescent due to the formation of a nonemissive ICT state after ESIPT.[39] The electron-withdrawing ability of the azole moiety increases with methylation, and hence, the ICT from the phenolic moiety to the heterocyclic ring is favored more. Complex formation reduces the interaction of the water molecule with the pyridine nitrogen, such as reduction in hydrogen bonding should reduce the electron-withdrawing ability of the azole moiety. The difference in behavior of HPIP-b and HPIP-c is due to the position of the pyridine nitrogen atom. As shown in Figure 5 (see section 3.5 for the orientation), the hydrogen bonding of the rim hydroxyl group/water molecule with pyridine nitrogen is less feasible in the HPIP-b complex than in the HPIP-c complex. The nonradiative decay increases upon protonation at the pyridine nitrogen.[36,37,67] Therefore, the larger decrease in the non-radiative decay in HPIP-b than that in HPIP-c may be due to higher reduction in hydrogen bonding with pyridine nitrogen.

Figure 6 depicts the fluorescence spectra of HPBI, HPIP-b, and HPIP-c in DMSO at different concentrations of β-CD. As in an aqueous medium in DMSO, HPBI also exhibits dual emission due to normal and tautomer fluorescence (Figure 6a). The intensities of both the bands increase with β-CD concentration up to 11 mM. With a further increase in β-CD concentration, the intensity of the tautomer emission increases with an increase in β-CD concentration. However, that of normal emission decreases above 11 mM, and a new band starts to appear at 415 nm. The intensity of the new band increases with β-CD concentration. On the other hand, in both HPIP-b and HPIP-c, the additional band appears as a shoulder in between the normal and tautomer bands even in the absence of β-CD. With an increase in β-CD, the tautomer emission undergoes a blue shift with an increase in intensity, and the new band is buried underneath of the tautomer band. These changes suggest that in DMSO also, the ESIPT process is favored more upon formation of an inclusion complex. The normal emission intensity decreases, and quasi-isoemissive points are observed. The presence of quasi-isoemissive points indicates the equilibrium between *trans*-enol and the anion. The absence of a quasi-isoemissive point in HPBI (Figure 6a) is due to the complicated nature of the equilibrium, that is, the absence of an anion at lower concentration, where the decrease in the nonradiative decay from *trans*-enol dominates over other factors, and the formation of an anion only at higher concentration.

To confirm the origin of the emitting species, the fluorescence excitation spectra of all three molecules are recorded in DMSO at different concentrations of β-CD (Figures 7−9). The excitation spectra monitored at the normal emission (Figures 7a, 8a, and 9a) are blue-shifted from the excitation spectra monitored at the tautomer emission (Figures 7c, 8c, and 9c). This indicates that the normal and tautomer emissions originate from two distinct ground-state species, *trans*- and *cis*-enols, respectively. The red-shifted absorption band at around 365 nm is present only in the excitation spectra monitored at 420 (Figure 7b), 415 (Figure 8b), and 430 nm (Figure 9b). These show that the new band is due to different species. It can be assigned to a monoanion formed by the deprotonation of a phenolic proton. This is supported by the

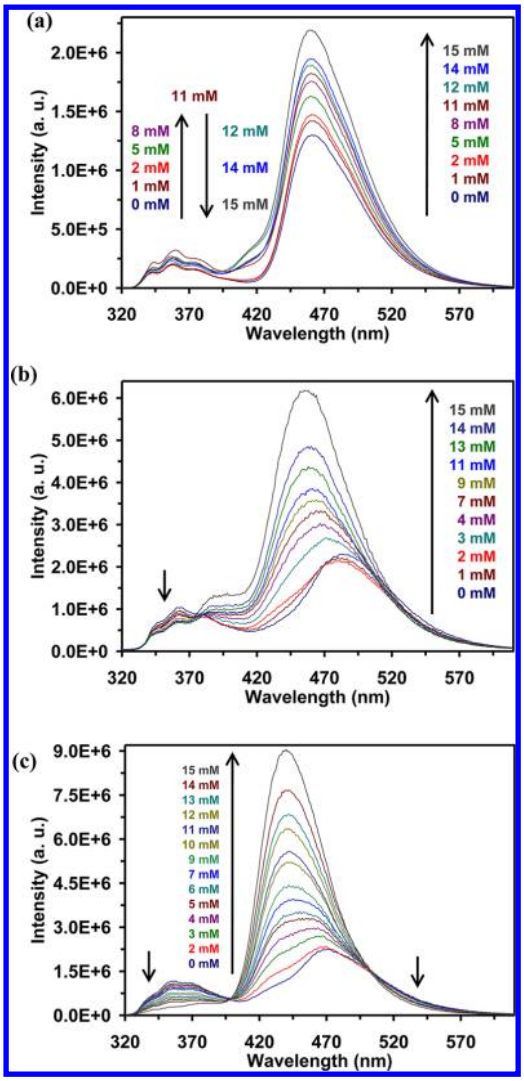

Figure 6. Fluorescence spectra of (a) HPBI, (b) HPIP-b, and (c) HPIP-c in DMSO as a function of [β-CD].

following facts: (i) the red shift is observed in the absorption and the excitation spectra upon deprotonation in HPBI and its analogues HPIP-b and HPIP-c, and the new band absorption spectrum is close to that of monoanion absorption spectrum (see later); (ii) the positions of the bands are consistent with the fact that the monoanion fluorescence spectrum is red-shifted with respect to the normal emission and blue-shifted compared to the tautomer emission.

DMSO acts as proton acceptor, and it can abstract the proton from a hydrogen bond donor depending on the acidity of the donor. The resulting anion is stabilized by solvation (Chart 1). The monoanion is formed in a nitrogen-substituted analogue even in the absence of β-CD but not in HPBI due to greater stabilization of the monoanionic form of HPIP-b and HPIP-c than the monoanionic form of HPBI due to the presence of a pyridine nitrogen. This was substantiated by the lower p*K*a of HPIP-b and HPIP-c than that of HPBI.[25,36,37] The pK_a value of HPBI decreases inside of the β-CD due to stabilization of the monoanion by the β-CD nanocavity; therefore, addition of β-CD leads to formation of a monoanion in HPBI.

The formation of the monoanion was further substantiated by fluorescence decay measurements. The lifetime data of

dx.doi.org/10.1021/jp311438s | J. Phys. Chem. A 2013, 117, 4084−4095

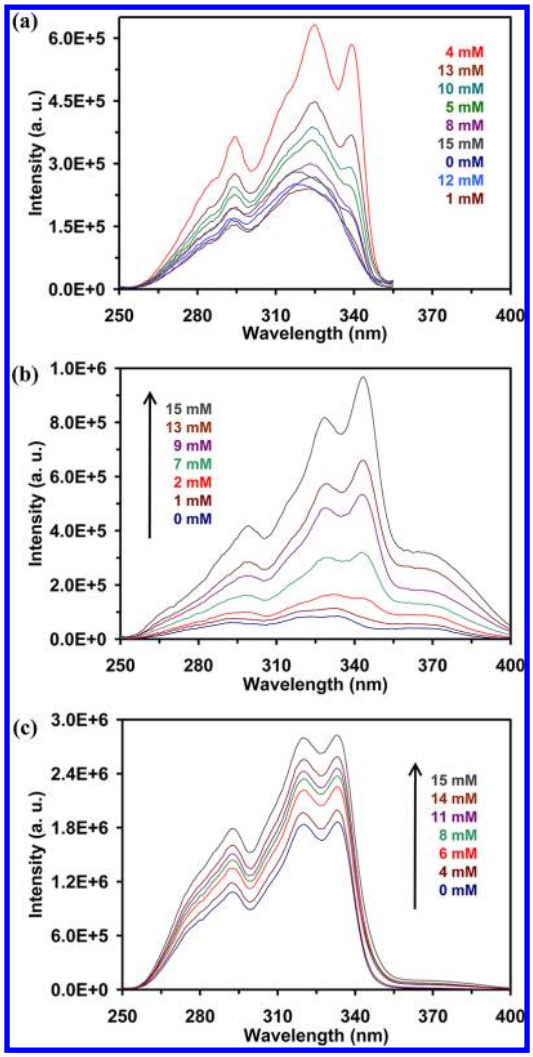

Figure 7. Fluorescence excitation spectra of HPBI in DMSO with increasing concentrations of β-CD monitored at (a) 355, (b) 420, and (c) 465 nm.

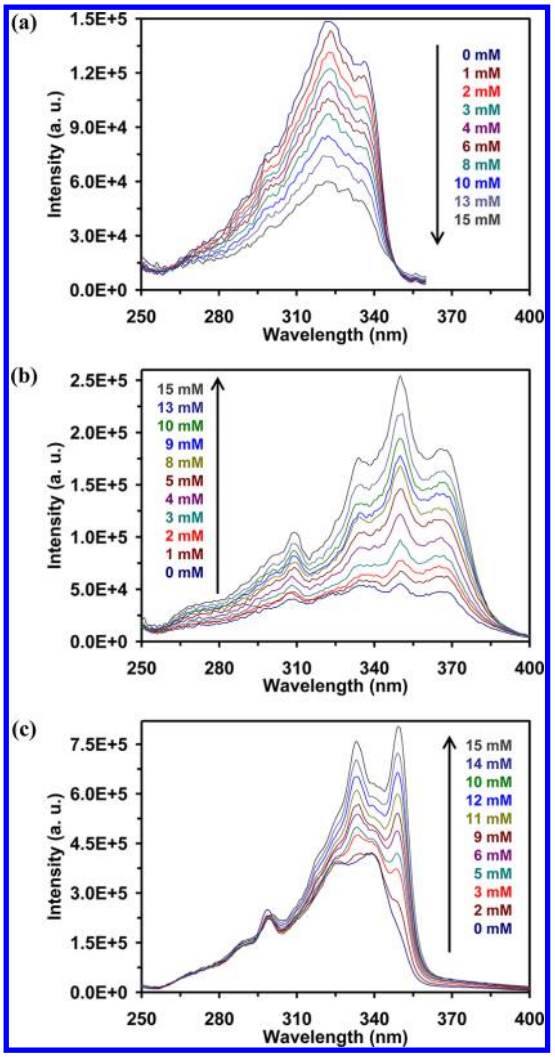

Figure 8. Fluorescence excitation spectra of HPIP-b in DMSO with increasing concentrations of β-CD monitored at (a) 365, (b) 415, and (c) 485 nm.

HPBI, HPIP-b, and HPIP-c in DMSO in the presence and absence of β-CD are tabulated in Table 1. The lifetimes of the normal emission of the fluorophores are not affected by the presence of β-CD. Though the lifetime of the tautomer emission of HPBI is not affected by β-CD, there is an increase in the lifetime of the tautomer emission of HPIP-b and HPIP-c. Using a 375 nm laser diode as the excitation source, the decay was monitored at 420, 435, and 438 nm for HPBI, HPIP-b, and HPIP-c, respectively. The lifetime values thus obtained are different from those of the normal and tautomer emissions. This confirms the formation of a monoanion.

3.3. Binding Constant. To determine the stoichiometry and the binding constant of the inclusion complexes, the fluorescence intensities of the tautomer emissions at different β-CD concentrations in water as well as DMSO were analyzed using Benesi–Hildebrand equations[73] (eq 1) for 1:1 complex formation.

$$\frac{1}{I - I_0} = \frac{1}{I_\alpha - I_0} + \frac{1}{(I_\alpha - I_0)K[\mathrm{CD}]} \quad (1)$$

where I_0, I, and I_∞ are emission intensities in the absence of β-CD, at an intermediate β-CD concentration, and when the molecule is completely encapsulated in β-CD, respectively, and K is the association constant.

The plot of $1/(I - I_0)$ against $[\beta\text{-CD}]^{-1}$ shows linear variation, justifying the validity of eq 1 and thus showing the formation of a 1:1 complex between the fluorophores and β-CD both in water and in DMSO. The plots of $1/(I - I_0)$ against $[\beta\text{-CD}]^{-2}$ could not be fitted linearly (not shown) for all of the solutions, which rules out the 1:2 complex formation with β-CD. The association constants obtained from the Benesi–Hildebrand plot for HPIP-b and HPIP-c with β-CD in water are 200 and 95 M^{-1}, respectively. Warner and his group calculated the binding constant for HPBI/β-CD inclusion complex formation to be 131 M^{-1} in water.[21] In DMSO, association constants for HPBI, HPIP-b, and HPIP-c are 193, 78, and 70 M^{-1}, respectively.

3.4. pH Titration. The prototropic equilibrium of the fluorophores is affected by complexation and the calculation of acidity constants (pK_a), which gives useful information about guest orientation inside of the inclusion complex.[21,74,75] Hence, the acidity constants (pK_a) of HPIP-b and HPIP-c in the presence of β-CD (15 mM) were determined spectrophotometrically with the help of UV–visible absorption measurements at different pHs in aqueous β-CD solutions (Figure 10).

dx.doi.org/10.1021/jp311438s | J. Phys. Chem. A 2013, 117, 4084–4095

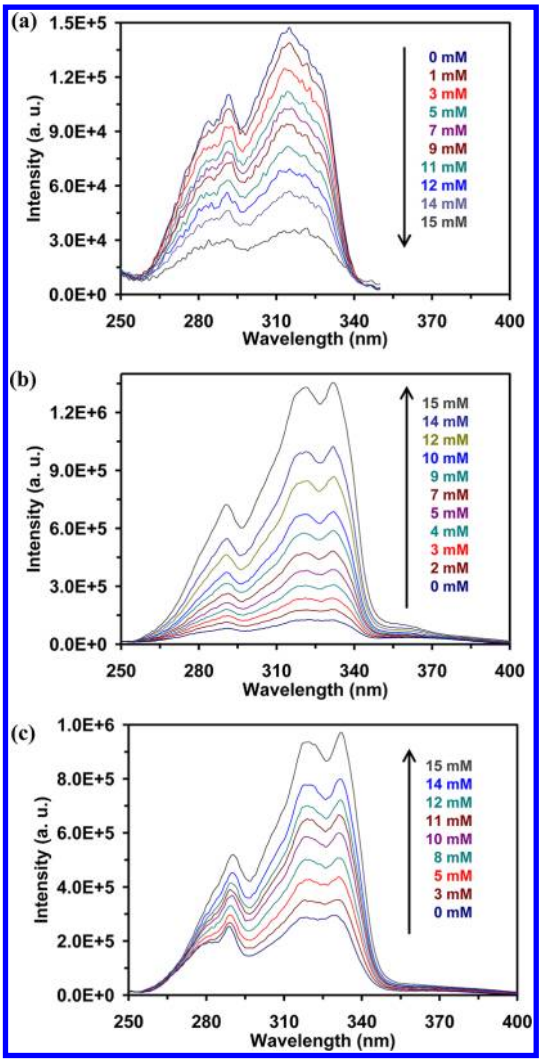

Figure 9. Fluorescence excitation spectra of HPIP-c in DMSO with increasing concentrations of β-CD monitored at (a) 355, (b) 430, and (c) 465 nm.

Chart 1. Solvated Structures

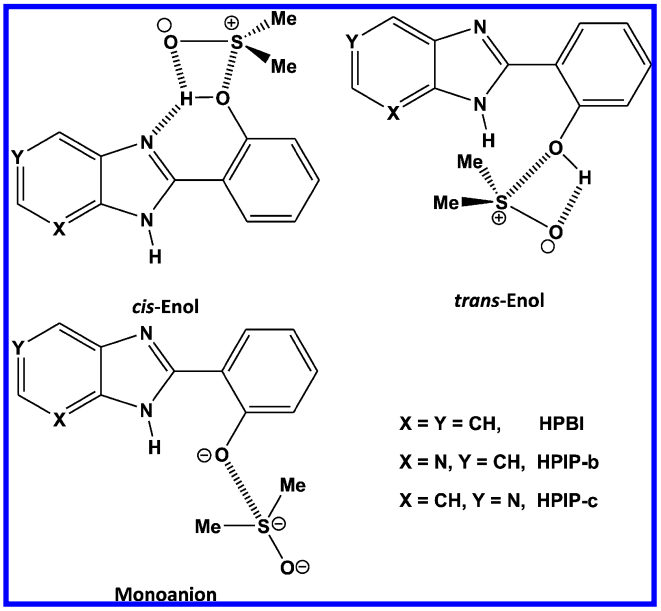

Table 1. Lifetimes of HPBI, HPIP-b, and HPIP-c in the Absence and Presence of β-CD (15 mM) in DMSO

	normal emission[a]		tautomer emission[a]		anion emission[b]	
sample	τ_1^N (ns)	χ^2	τ_1^T (ns)	χ^2	τ_1^A (ns)	χ^2
HPBI						
DMSO	1.5	1.0	4.4	1.0		
DMSO + β-CD	1.5	1.0	4.4	1.0	3.2	1.0
HPIP-b						
DMSO	1.2	1.0	3.2	1.1	4.0	1.1
DMSO + β-CD	1.2	1.1	3.5	1.2	4.1	1.0
HPIP-c						
DMSO	1.2	1.0	3.4	1.1	3.7	1.0
DMSO + β-CD	1.2	1.0	3.9	1.0	3.9	1.0

[a] λ_{exc} = 308 nm. [b] λ_{exc} = 375 nm.

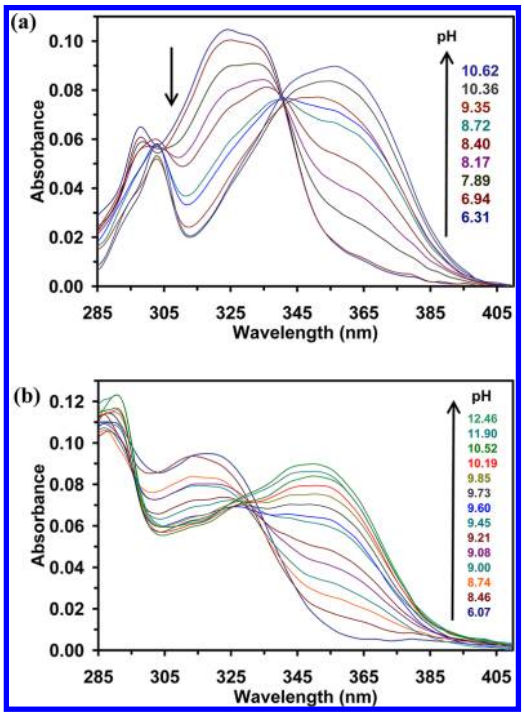

Figure 10. Absorption spectra of (a) HPIP-b and (b) HPIP-c in 15 mM aqueous β-CD at different pHs.

In the presence of β-CD, HPIP-b is completely in the neutral form at pH 6.3, while HPIP-c is neutral at pH 5.3. The pK_a value for the neutral−monoanion equilibrium of HPIP-b was found to be 8.3, which is a little lower than 8.6 in the absence of β-CD reported by Dogra et al.[36] In the case of HPIP-c, also the pK_a value for the neutral−monoanion equilibrium (8.6) is lower than that in aqueous solution (9.3).[37]

The fluorophores have two acidic centers, namely, the phenolic OH and the imidazole NH. Phenol has pK_a ≈ 10, while imidazole has pK_a ≈ 14.5. Hence, because the observed p*K*a is closer to that of phenol, the monoanion formed is due to the deprotonation of phenolic OH. The lower pK_a value observed here compared to that of phenol (∼10) may be due to polarization of the phenolic OH bond as a result of the presence of an electron-withdrawing imidazopyridine moiety. Because the pK_a of the imidazole >NH group is higher than that of the hydroxyl proton of the β-CD,[7,8] we did not attempt to calculate the pK_a of the imidazole >NH group.

dx.doi.org/10.1021/jp311438s | J. Phys. Chem. A 2013, 117, 4084−4095

A similar decrease in pK_a values was observed for 2-(2′-hydrophenyl)benzazoles[21] and other aromatic alcohols.[76] The lowering of the pK_a value for the neutral−monoanion in the presence of β-CD is ascribed to the formation of an intermolecular hydrogen bond between the phenolic oxygen and the alcoholic OH groups of β-CD, the alcoholic OH groups acting as the H-bond donor. This facilitates the stabilization of the monoanion formed by deprotonation. The difference in the pK_a values in the presence and absence of β-CD is a measure of the strength of the intramolecular hydrogen bond through which the ESIPT occurs. It appears that the strength of the intramolecular hydrogen bond depends on the position of the pyridine nitrogen and is stronger in HPIP-c than that in HPIP-b. This was consistent with the fact that Φ_T/Φ_N is higher in HPIP-c than that in HPIP-b (Figure 4).

3.5. Orientations of the Guests in Inclusion Complexes and NMR Studies. The length and the interior diameter of the β-CD cavity are 7.9 and 7.8 Å, respecively.[77] The dimensions of the density functional theory (DFT)-optimized structure HPIP-b using the method B3LYP/6-31G(d) by Gaussian 03 software[78] are shown in Figure 11.[53]

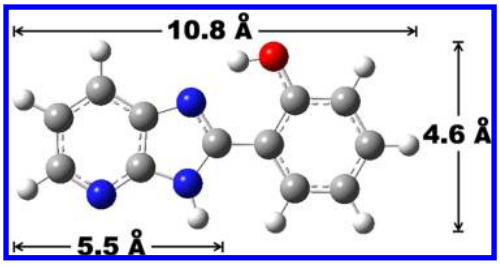

Figure 11. Optimized geometry of HPIP-b obtained from DFT calculations.

The dimensions of HPBI and HPIP-c are nearly the same as those of HPIP-b.[53] On the basis of the dimensions of the host and guest molecules, it can be inferred that the guest can be encapsulated only partially, and the guest molecule can enter the cavity of β-CD in two possible ways, as shown schematically in Figure 12. If the guests were oriented as shown in Figure 12a, the −OH group of the guest molecules would be present near the rim. On the other hand, if the guests were present in the reverse way as shown in Figure 12b, the −OH group of the guest molecules would be present inside of the cavity. Because the interior of the CD nanocavity is hydrophobic, the formation of the monoanion is possible only if the solvent molecule interacts with guest molecules. The formation of the monoanion clearly suggests that the phenyl ring of the molecule is present outside of the cavity (Figure 12a). Such an orientation allows restricted hydrogen bonding with solvent molecules. It is also feasible for intermolecular H-bonding with the OH of β-CD.

Formation of the monoanion indicates that HPIP-b and HPIP-c partially penetrate the β-CD cavity with the imidazopyridine moiety. The phenolic group resides outside of the upper rim are exposed to the solvent environment, and its OH group presents near the rim. HPBI was also reported to have the same orientation in aqueous β-CD.[21]

The NMR spectra of the guest in the presence and absence of β-CD should give a clearer picture of the orientation of the molecules inside of the β-CD cavity.[11] Due to poor solubility, we are not able to record the NMR in heavy water. However, ^{1}H NMR spectra were recorded in DMSO, and the aromatic region of the spectra is depicted in Figure 13. NMR decoupling experiments were performed for proton peak assignments (Supporting Information). In all three molecules, as expected, the complexation with β-CD affects protons of the benzimidazole/pyridoimidazole more than the protons of the hydroxyphenyl ring. In HPBI (Figure 13a), both H_a and H_b protons appears as doublets, in the absence of β-CD, but peaks of both protons are shifted and merged to appear as a broad singlet at δ 7.653 in the presence of β-CD. Similarly, the H_b and $H_{b'}$ peaks appear as pseudo-triplets at δ 7.286 in the absence of β-CD, but the splitting disappears to a singlet at 7.277 in the presence of β-CD. On the other hand, the effect is negligible in peaks of phenolic ring protons. The chemical shift values for HPIP-b are in the order $H_e < H_g < H_b < H_f < H_a < H_d < H_c$ (Figure 13b). In the absence of β-CD, the H_a proton peak appears as a doublet at 8.06 ppm, and the H_d proton peak appears as a doublet at 8.10 ppm. In the presence of β-CD, the H_d proton is affected less, but H_a proton peaks are shifted downfield and merged with the H_d proton to appear as a broad shoulder. The H_c proton appears as a doublet in the absence of β-CD and merges to appear as a broad single peak in the presence of β-CD. The well-resolved peaks of the H_b proton in the absence of β-CD become less resolved in the presence of β-CD. However, the effect of β-CD complexation is negligible for protons of the phenolic ring. Similarly, in the case of HPIP-c, the chemical shift values of H_a are shifted from 8.947 to 8.930, H_b is shifted from 8.290 to 8.281, and H_c is shifted from 7.687 to 7.680 in the presence of β-CD. As expected, the shift is more in H_a than that in H_b or H_c. The effect of CD complexation is also less on phenolic ring protons (Figure 13c).

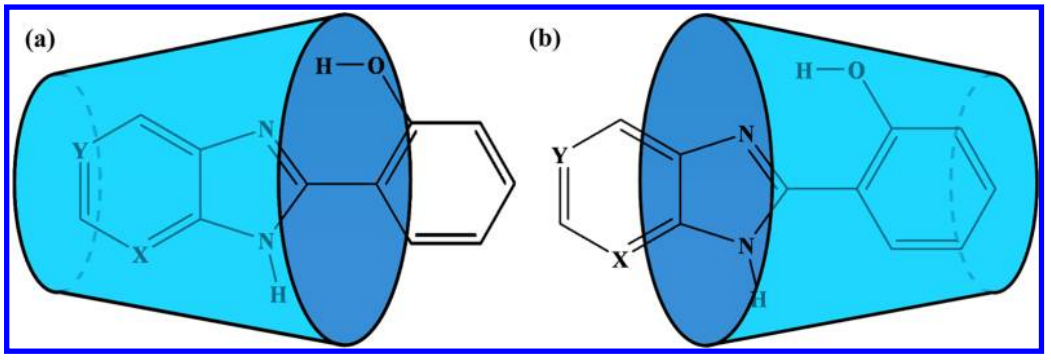

Figure 12. Mode of 1:1 complexation of HPIP-b with β-CD with the heterocyclic imidazopyridine moiety (a) inside and (b) outside of the β-CD nanocavity.

dx.doi.org/10.1021/jp311438s | J. Phys. Chem. A 2013, 117, 4084−4095

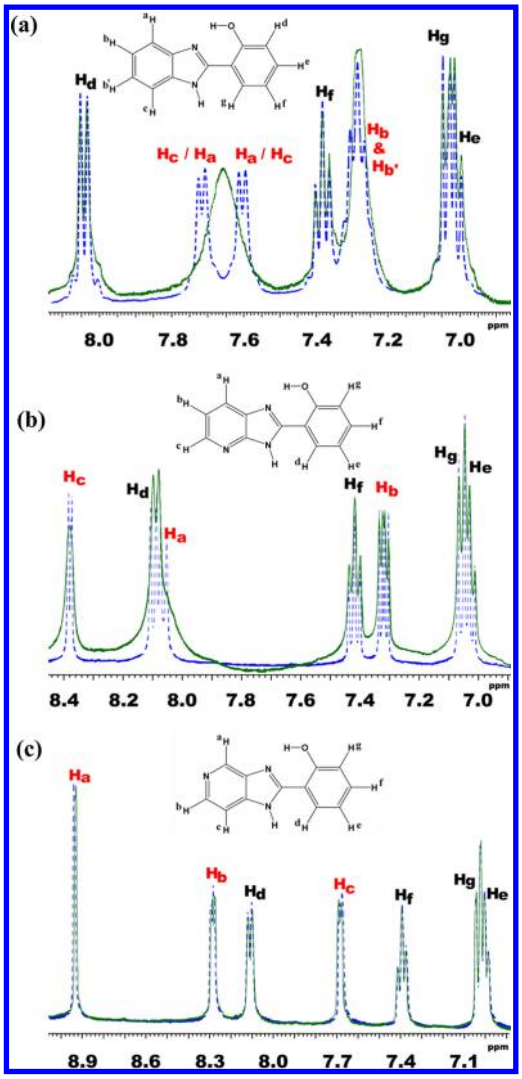

Figure 13. ^{1}H NMR spectra of (a) HPBI, (b) HPIP-b, and (c) HPIP-c in the presence (solid line) and absence (dotted line) of β-CD in DMSO-d_6.

HPIP-b and HPIP-c monocations are formed by the protonation of the ring nitrogen.[36,37] Therefore, to substantiate further, the fluorescence characteristics of monocationic forms of HPIP-b and HPIP-c are measured as a function of β-CD concentration in aqueous solutions. The fluorescence spectra of the monocations are unaffected by β-CD (Supporting Information Figure S18). This suggested that the monocations are not forming a complex with β-CD. On the other hand, monocationic forms of 4′-*N*,*N*-dimethylamino-substituted analogues 2-(4′-*N*,*N*-dimethylaminophenyl)imidazopydridines form an inclusion complex with β-CD.[11,61] The mode of encapsulation of 4′-*N*,*N*-dimethylamino-substituted analogues is different from that of HPIP-b and HPIP-c. The 4′-*N*,*N*-dimethylaminophenyl is encapsulated, and the benzimidazole/imidazopyridine ring is present outside of the cavity.[11,61,79] In 4′-*N*,*N*-dimethylamino analogues, also the monocations are formed by protonation of heterocylic ring nitrogen. Because the cationic part of the molecule is present outside of the cavity, the cation binds with the β-CD cavity, and the solvation shell around the cationic heterocyclic ring is intact. On the other hand, in HPIP-b or HPIP-c, the heterocyclic ring enters the hydrophobic cavity; this will remove the shell solvation around the imidazopyridine ring. Consequently, monocations are not encapsulated inside of the hydrophobic CD cavity. Douhal et al. also demonstrated that ESIPT exhibiting milrinone also enters the CD cavity through the pyridine ring.[80] It appears that substitution influences the orientation of the molecules.

4. CONCLUSION

HPBI, HPIP-b, and HPIP-c enter the β-CD cavity through the benzimidazole/imidazopyridine moiety. NMR confirms the proposed orientation of the molecules. Encapsulation of HPIP-b and HPIP-c by β-CD enhanced the ESIPT reaction. Though all three molecules form 1:1 inclusion complexes with β-CD, the effects of β-CD on HPIP-b and HPIP-c are much more significant compared to that of HPBI. Remarkable enhancement in the fluorescence and a red shift are observed in the tautomer emission of HPIP-b and HPIP-c compared to that of HPBI. The tautomer emission is increased by both an ESIPT-favorable environment of the β-CD cavity and reduction in the torsional-induced nonradiative decay through a twisted ICT state. The pK_a for the neutral−monoanion equilibrium of the molecules decreases due to greater stabilization of the monoanion inside of the nanocavity. All three molecules donate the proton to DMSO to form a monoanion in DMSO. The monoanion of HPBI is formed in DMSO solution above 4 mM β-CD. However, the presence of extra nitrogen stabilizes the monoanion, and HPIP-b and HPIP-c are present as both a neutral and monoanion in the presence as well as absence of β-CD in DMSO. The presence of extra nitrogen makes HPIP-b and HPIP-c more sensitive to the environment than HPBI, and therefore, they can be a better environment probe than HPBI. Unlike the neutral and monoanion, monocations of HPIP-b and HPIP-c do not form a complex with β-CD.

■ ASSOCIATED CONTENT

Ⓢ Supporting Information

^{1}H and ^{13}C NMR, IR spectra of HPBI, HPIP-b, and HPIP-c, decoupled NMR and assignment of NMR peaks, dielectric constant determination plots, time-resolved fluorescence decays, Benesi−Hildebrand plots, NMR titration spectra, and the fluorescence of monocationic forms at different CD concentrations. This material is available free of charge via the Internet at http://pubs.acs.org.

■ AUTHOR INFORMATION

Corresponding Author

*Phone: +91-3612582315. Fax +91-3612582349. E-mail: gkrishna@iitg.ernet.in.

Notes

The authors declare no competing financial interest.

■ ACKNOWLEDGMENTS

The authors acknowledge the Department of Science and Technology (DST), India and the Council of Scientific and Industrial Research (CSIR), India for financial support. Central Instrumental Facility (CIF), IIT Guwahati is acknowledged for the TCSPC and the proton NMR instruments and Gauhati University for the ^{13}C NMR spectral measurements. The authors thank Dr. M. Hormi of Gauhati University for helping obtain the ^{13}C NMR. F.A.S.C. and S.K.B. thank CSIR for research fellowships.

DEDICATION

[#]Dedicated to Prof. Jack Saltiel on his 75th birthday.

REFERENCES

(1) Rekharsky, M. V.; Inoue, Y. Complexation Thermodynamics of Cyclodextrins. *Chem. Rev.* **1998**, *98*, 1875−1918.
(2) Villalonga, R.; Cao, R.; Fragoso, A. Supramolecular Chemistry of Cyclodextrins in Enzyme Technology. *Chem. Rev.* **2007**, *107*, 3088−3116.
(3) Ukeama, K.; Hirayama, F.; Irie, T. Cyclodextrin Drug Carrier Systems. *Chem. Rev.* **1998**, *98*, 2045−2076.
(4) Breslow, R.; Dong, S. D. Biomimetic Reactions Catalyzed by Cyclodextrins and Their Derivatives. *Chem. Rev.* **1998**, *98*, 1997−2011.
(5) Harada, A. Cyclodextrin-Based Molecular Machines. *Acc. Chem. Res.* **2001**, *34*, 456−464.
(6) Hashimoto, S.; Thomas, J. K. Fluorescence Study of Pyrene and Naphthalene in Cyclodextrin−Amphiphile Complex Systems. *J. Am. Chem. Soc.* **1985**, *107*, 4655−4662.
(7) Blyshak, L. A.; Rossi, T. M.; Patonay, G.; Warner, I. M. Cyclodextrin-Modified Solvent Extraction for Polynuclear Aromatic Hydrocarbons. *Anal. Chem.* **1988**, *60*, 2127−2131.
(8) Iglesias, E. Inclusion Complexation of Novocaine by in Aqueous Solutions. *J. Org. Chem.* **2006**, *71*, 4383−4392.
(9) Banerjee, A.; Basu, K.; Sengupta, P. K. Effect of β-Cyclodextrin Nanocavity Confinement on the Photophysics of Robinetin. *J. Photochem. Photobiol., B* **2007**, *89*, 88−97.
(10) Sanz, M.; Organero, J. A.; Douhal, A. Proton and Charge Transfer Reactions Dynamics of a Hydroxyflavone Derivative in a Polar Solvent and in a Cyclodextrin Nanocavity. *Chem. Phys.* **2007**, *338*, 135−142.
(11) Dash, N.; Chipem, F. A. S.; Krishnamoorthy, G. Encapsulation of 2-(4′-*N*,*N*-Dimethylamino)phenylimidazo[4,5-*b*]pyridine in β-Cyclodextrin: Effect on H-Bond-induced Intramolecular Charge Transfer Emission. *Photochem. Photobiol. Sci.* **2009**, *8*, 1708−1715.
(12) Das, P.; Chakrabarty, A.; Haldar, B.; Mallick, A.; Chattopadhyay, N. Effect of Cyclodextrin Nanocavity Confinement on the Photophysics of a β-Carboline Analogue: A Spectroscopic Study. *J. Phys. Chem. B* **2007**, *111*, 7401−7408.
(13) Matsushita, Y.; Suzuki, T.; Ichimura, T.; Hikida, T. Cavity Size Effect on the Excited State Dynamics of Methyl 4-(Dimethylamino)-benzoate−Cyclodextrin Complexes. *J. Phys. Chem. A* **2004**, *108*, 7490−7496.
(14) Ralkshit, S.; Vasudevan, S. Resonance Energy Transfer from β-Cyclodextrin-Capped ZnO:MgO Nanocrystals to Included Nile Red Guest Molecules in Aqueous Media. *ACS Nano* **2008**, *2*, 1473−1479.
(15) Faiz, J. A.; Kyllonen, L. E. P.; Contreras-Carballada, P.; Williams, R. M.; De Cola, L.; Pikramenou, Z. Photoinduced Energy Transfer Across Non-Covalent Bonds in the Nanoscale: Cyclodextrin Hosts with Enhanced Luminescent Properties for Guest Communication. *Dalton Trans.* **2009**, 3980−3987.
(16) Douhal, A. Ultrafast Guest Dynamics in Cyclodextrin Nanocavities. *Chem. Rev.* **2004**, *104*, 1955−1976.
(17) Martín, C.; Gil, M.; Cohen, B.; Douhal, A. Ultrafast Photodynamics of Drugs in Nanocavities: Cyclodextrins and Human Serum Albumin Protein. *Langmuir* **2012**, *28*, 6746−6759.
(18) D'Souza, R. N.; Pischel, U.; Nau, W. M. Fluorescent Dyes and Their Supramolecular Host/Guest Complexes with Macrocycles in Aqueous Solution. *Chem. Rev.* **2011**, *111*, 7941−7980.
(19) Wagner, B. D. Hydrogen Bonding of Excited States in Supramolecular Host−Guest Inclusion Complexes. *Phys. Chem. Chem. Phys.* **2012**, *14*, 8825−8835.
(20) Roberts, E. L.; Chou, P. T.; Alexander, T. A.; Agbaris, R. A.; Warner, I. M. Effects of Organized Media on the Excited-State Intramolecular Proton Transfer of 1O-Hydroxybenzo[*h*]quinoline. *J. Phys. Chem.* **1995**, *99*, 5431−5437.
(21) Roberts, E. L.; Dey, J.; Warner, I. M. Excited-State Intramolecular Proton Transfer of 2-(2′-Hydroxyphenyl)benzimidazole in Cyclodextrins and Binary Solvent Mixtures. *J. Phys. Chem. A* **1997**, *101*, 5296−5301.
(22) Paul, B. K.; Samanta, A.; Guchhait, N. Modulation of Excited-State Intramolecular Proton Transfer Reaction of 1-Hydroxy-2-naphthaldehyde in Different Supramolecular Assemblies. *Langmuir* **2010**, *26*, 3214−3224.
(23) Roberts, E. L.; Dey, J.; Warner, I. M. Ground- and Excited-State Structural Orientation of 2-(2′-Hydroxyphenyl)benzazoles in Cyclodextrins. *J. Phys. Chem.* **1996**, *100*, 19681−19686.
(24) Sarkar, N.; Das, K.; Das, S.; Datta, A.; Nath, D.; Bhattacharyya, K. Excited-State Intramolecular Proton Transfer of 2-(2′-Hydroxyphenyl)benzimidazole in Micelles. *J. Phys. Chem.* **1995**, *99*, 17711−17714.
(25) Sinha, H. K.; Dogra, S. K. Ground and Excited State Prototropic Reactions in 2-(*o*-Hydroxyphyenyl)benzimidazole. *Chem. Phys.* **1986**, *102*, 337−347.
(26) Penedo, J. C.; Mosquera, M.; Rodríguez-Prieto, F. Role of Hydrogen-Bonded Adducts in Excited-State Proton-Transfer Processes. *J. Phys. Chem. A* **2000**, *104*, 7429−7441.
(27) Mosquera, M.; Penedo, J. C.; Rodríguez, M. C. R.; Rodríguez-Prieto, F. Photoinduced Inter- and Intramolecular Proton Transfer in Aqueous and Ethanolic Solutions of 2-(2′-Hydroxyphenyl)-benzimidazole: Evidence for Tautomeric and Conformational Equilibria in the Ground State. *J. Phys. Chem.* **1996**, *100*, 5398−5407.
(28) Douhal, A.; Amat-Guerri, F.; Lillo, M. P.; Acuña, A. U. Proton Transfer Spectroscopy of 2-(2′-Hydroxyphenyl)imidazole and 2-(2′-Hydroxyphenyl)benzimidazole Dyes. *J. Photochem. Photobiol., A* **1994**, *78*, 127−138.
(29) Das, K.; Sarkar, N.; Majumdar, D.; Bhattacharyya, K. Excited-State Intramolecular Proton Transfer and Rotamerism of 2-(2′-Hydroxyphenyl)benzimidazole. *Chem. Phys. Lett.* **1992**, *198*, 443−448.
(30) Das, K.; Sarkar, N.; Ghosh, A. K.; Majumdar, D.; Nath, D. N.; Bhattacharyya, K. Excited-State Intramolecular Proton Transfer in 2-(2-Hydroxyphenyl)benzimidazole and -benzoxazole: Effect of Rotamerism and Hydrogen Bonding. *J. Phys. Chem.* **1994**, *98*, 9126−9132.
(31) Ríos, M. A.; Ríos, M. C. Ab Initio Study of the Hydrogen Bond and Proton Transfer in 2-(2′-Hydroxyphenyl)benzothiazole and 2-(2′-Hydroxyphenyl)benzimidazole. *J. Phys. Chem. A* **1998**, *102*, 1560−1567.
(32) Williams, D. L.; Heller, A. Intramolecular Proton Transfer Reactions in Excited Fluorescent Compounds. *J. Phys. Chem.* **1970**, *74*, 4473−4480.
(33) Purkayastha, P.; Chattopadhyay, N. Role of Rotamerisation and Excited State Intramolecular Proton Transfer in the Photophysics of 2-(2′-Hydroxyphenyl)benzoxazole, 2-(2′-Hydroxyphenyl)benzimidazole and 2-(2′-Hydroxyphenyl)benzothiazole: A Theoretical Study. *Phys. Chem. Chem. Phys.* **2000**, *2*, 203−210.
(34) Vázquez, S. R.; Rodríguez, C. R.; Mosquera, M.; Rodríguez-Prieto, F. Excited-State Intramolecular Proton Transfer in 2-(3′-Hydroxy-2′-pyridyl)benzoxazole. Evidence of Coupled Proton and Charge Transfer in the Excited State of Some *o*-Hydroxyarylbenzazoles. *J. Phys. Chem. A* **2007**, *111*, 1814−1826.
(35) Krishnamoorthy, G.; Dogra, S. K. Excited State Intramolecular Proton Transfer in 2-(2′-Hydroxyphenyl)-3*H*-imidazo[4,5-*b*]pyridine: Effect of Solvents. *J. Lumin.* **2001**, *92*, 91−102.
(36) Krishnamoorthy, G.; Dogra, S. K. Prototropic Reactions of 2-(2′-Hydroxyphenyl)-3*H*-imidazo[4,5-*b*]pyridine in Aqueous and Organic Solvents. *J. Lumin.* **2001**, *92*, 103−114.
(37) Balamurali, M. M.; Dogra, S. K. Excited State Intramolecular Proton Transfer in 2-(2′-Hydroxyphenyl)-1*H*-imidazo[4,5-*c*]pyridine: Effects of Solvents. *J. Photochem. Photobiol., A* **2002**, *154*, 81−92.
(38) Rodríguez-Prieto, F.; Rodríguez, M. C. R.; González, M. M.; Fernández, M. A. R. Ground- and Excited-State Tautomerism in 2-(3′-Hydroxy-2′-pyridyl)benzimidazole. *J. Phys. Chem.* **1994**, *98*, 8666−8672.
(39) Brenlla, A.; Veiga, M.; Rodríguez, M. C. R.; Mosquera, M.; Rodríguez-Prieto, F. Fluorescence of Methylated Derivatives of Hydroxyphenylimidazopyridine. Resolution of Strongly Overlapping

Spectra and a New ESIPT Dye Showing Very Efficient Radiationless Deactivation. *Photochem. Photobiol. Sci.* **2011**, *10*, 1622−1636.
(40) Dogra, S. K. Spectral Characteristics of 2-(2′-Hydroxy-3′-pyridyl)benzimidazole: Effects of Solvents and Acid or Base Concentrations. *J. Mol. Struct.* **2005**, *734*, 51−60.
(41) Xiao, D.; Zhang, G.; Wang, H.; Tang, G.; Chen, W. Investigation on Nonlinear Transmission Property of Excited State Proton Transfer Molecule 2-(2′-Hydroxyphenyl)benzoxazole. *J. Nonlinear Opt. Phys. Mater.* **2000**, *9*, 309−314.
(42) Hillebrand, S.; Segala, M.; Buckup, T.; Correia, R. R. B.; Horowitz, F.; Stefani, V. First Hyperpolarizability in Proton-Transfer Benzoxazoles: Computer-Aided Design, Synthesis and Study of a New Model Compound. *Chem. Phys.* **2001**, *273*, 1−10.
(43) Sakai, K.-I.; Tsuzuki, T.; Itoh, Y.; Ichikawa, M.; Taniguchi, Y. Using Proton-Transfer Laser Dyes for Organic Laser Diodes. *Appl. Phys. Lett.* **2005**, *86*, 081103.
(44) Kasha, M. Proton-Transfer Spectroscopy. Perturbation of the Tautomerization Potential. *J. Chem. Soc., Faraday Trans. 2* **1986**, *82*, 2379−2392.
(45) Formosinho, S. J.; Arnaut, L. G. Excited-State Proton Transfer Reactions II. Intramolecular Reactions. *J. Photochem. Photobiol., A* **1993**, *75*, 21−48.
(46) Waluk, J. Conformational Aspects of Intra- and Intermolecular Excited-State Proton Transfer. In *Conformational Analysis of Molecules in Excited States*; Waluk, J., Ed.; Wiley-VCH: New York, 2000; Chapter 2, pp 57−112.
(47) Zhao, J.; Ji, S.; Chen, Y.; Guo, H.; Yang, P. Excited State Intramolecular Proton Transfer (ESIPT): From Principal Photophysics to the Development of New Chromophores and Applications in Fluorescent Molecular Probes and Luminescent Materials. *Phys. Chem. Chem. Phys.* **2012**, *14*, 8803−8817.
(48) Kwon, J. E.; Park, S. Y. Advanced Organic Optoelectronic Materials: Harnessing Excited-State Intramolecular Proton Transfer (ESIPT) Process. *Adv. Mater.* **2011**, *23*, 3615−3642.
(49) Hsieh, C.-C.; Jiang, C.-M.; Chou, P.-T. Recent Experimental Advances on Excited-State Intramolecular Proton Coupled Electron Transfer Reaction. *Acc. Chem. Res.* **2010**, *43*, 1364−1374.
(50) Sarkar, N.; Datta, A.; Das, S.; Das, K.; Bhattacharyya, K. Dual Emission of 2-(2′-Hydroxyphenyl)-benzimidazole in Reverse Micelle. *J. Photochem. Photobiol., A* **1997**, *109*, 259−265.
(51) Das, S. K.; Bansal, A.; Dogra, S. K. Excited State Intramolecular Proton Transfer Reactions in 2-(2-Hydroxyphenyl)benzimidazole in Micellar Solutions. *Bull. Chem. Soc. Jpn.* **1997**, *70*, 307−313.
(52) Chattopadhyay, N. Effect of Cyclodextrin Complexation on Excited State Proton Transfer Reactions. *J. Photochem. Photobiol., A* **1991**, *58*, 31−36.
(53) Chipem, F. A. S.; Krishnamoorthy, G. Comparative Theoretical Study of Rotamerism and Excited State Intramolecular Proton Transfer of 2-(2′-Hydroxyphenyl)benzimidazole, 2-(2′-Hydroxyphenyl)imidazo[4,5-*b*]pyridine, 2-(2′-Hydroxyphenyl)-imidazo[4,5-*c*]pyridine and 8-(2′-Hydroxyphenyl)purine. *J. Phys. Chem. A.* **2009**, *113*, 12063−12070.
(54) Chipem, F. A. S.; Nihar, D.; Krishnamoorthy, G. Role of Nitrogen Substitution in Phenyl Ring on Excited State Intramolecular Proton Transfer and Rotamerism of 2-(2′-Hydroxyphenyl)-benzimidazole: A Theoretical Study. *J. Chem. Phys.* **2011**, *134*, 104308.
(55) Mosquera, M.; Rodríguez, M. C. R.; Rodríguez-Prieto, F. Competition between Protonation and Deprotonation in the First Excited Singlet State of 2-(3′-Hydroxy-2′-pyridyl)benzimidazole in Acidic Solutions. *J. Phys. Chem. A* **1997**, *101*, 2766−2772.
(56) Rodríguez, M. C. R.; Mosquera, M.; Rodríguez-Prieto, F. Ground- and Excited-State Tautomerism in Anionic 2-(6′-Hydroxy-2′-pyridyl)benzimidazole: Role of Solvent and Temperature. *J. Phys. Chem. A* **2001**, *105*, 10249−10260.
(57) Chou, P. T.; Cooper, W. C.; Clements, J. H.; Studer, S. L.; Cheng, C. P. A Comparative Study. The Photophysics of 2-Phenylbenzoxazoles and 2-Phenylbenzothiazoles. *Chem. Phys. Lett.* **1993**, *216*, 300−304.
(58) LeGourriérec, D.; Kharlanov, V.; Brown, R. G.; Rettig, W. Excited-State Intramolecular Proton Transfer (ESIPT) in 2-(2′-Hydroxyphenyl)-oxazole and -Thiazole. *J. Photochem. Photobiol., A* **2000**, *130*, 101−111.
(59) Kharlanov, V. A.; Rettig, W.; Knyazhansky, M. I.; Makaraova, N. Multiple Emission of N-(1-Anthryl)-pyridinium. *J. Photochem. Photobiol., A* **1997**, *103*, 45−50.
(60) Chen, W.; Chang, C.-E.; Gilson, M. K. Calculation of Cyclodextrin Binding Affinities: Energy, Entropy, and Implications for Drug Design. *Biophys. J.* **2004**, *87*, 3035−3049.
(61) Krishnamoorthy, G.; Dogra, S. K. Twisted Intramolecular Charge Transfer of 2-(4′-*N*,*N*-Dimethylaminophenyl)pyrido[3,4-*d*]-imdazole in Cyclodextrins: Effect of pH. *J. Phys. Chem. A* **2000**, *104*, 2542−2551.
(62) Crosby, G. A.; Demas, J. N. Measurement of Photoluminescence Quantum Yields. Review. *J. Phys. Chem.* **1971**, *75*, 991−1024.
(63) Jiang, Y.-B. Effect of Cyclodextrin Inclusion Complex Formation on the Twisted Intramolecular Charge Transfer (TICT) of the Included Compound: The *p*-Dimethylaminobenzoic Acid-*β*-Cyclodextrin System. *J. Photochem. Photobiol., A* **1995**, *88*, 109−116.
(64) Panja, S.; Chowdhury, P.; Chakravorti, S. Modulation of Complexation of 4(1H-Pyrrole-1-yl)benzoic Acid with *β*-Cyclodextrin in Aqueous and Non-Aqueous Environments. *Chem. Phys. Lett.* **2004**, *393*, 409−415.
(65) Critchfield, F. E.; Gibson, J. A., Jr.; Hall, J. L. Dielectric Constant for the Dioxane—Water System from 20 to 35°. *J. Am. Chem. Soc.* **1953**, *75*, 1991−1992.
(66) Nigam, S.; Durocher, G. Spectral and Photophysical Studies of Inclusion Complexes of Some Neutral 3*H*-Indoles and Their Cations and Anions with *β*-Cyclodextrin. *J. Phys. Chem.* **1996**, *100*, 7135−7142.
(67) Brenlla, A.; Veiga, M.; Lustres, J. L. P.; Rodríguez, M. C. R.; Rodríguez-Prieto, F.; Mosquera, M. Photoinduced Proton and Charge Transfer in 2-(2′-Hydroxyphenyl)imidazo[4,5-b]pyridine. *J. Phys. Chem. B* **2013**, *117*, 884−896.
(68) Konoshima, H.; Nagao, S.; Kiyota, I.; Amimoto, K.; Yamamoto, N.; Sekine, M.; Nakata, M.; Furukawa, K.; Sekiya, H. Excited-State Intramolecular Proton Transfer and Charge Transfer in 2-(2′-Hydroxyphenyl)benzimidazole Crystals Studied by Polymorphs-Selected Electronic Spectroscopy. *Phys. Chem. Chem. Phys.* **2012**, *14*, 16448−16457.
(69) Douhal, A.; Fiebig, T.; Chachisvilis, M.; Zewail, A. H. Femtochemistry in Nanocavities: Reactions in Cyclodextrins. *J. Phys. Chem. A* **1998**, *102*, 1657−1660.
(70) Dash, N.; Chipem, F. A. S.; Swaminathan, R.; Krishnamoorthy, G. Hydrogen Bond Induced Twisted Intramolecular Charge Transfer in 2-(4′- Dimethylaminophenyl)imidazo[4,5-*b*]pyridine. *Chem. Phys. Lett.* **2008**, *460*, 119−124.
(71) Krishnamoorhy, G. Hydrogen Bonding Effects On Intramolecular Charge Transfer. In *Hydrogen Bonding and Transfer in the Excited State*; Han, K.-L., Zhao, G. J., Eds.; John Wiley & Sons Ltd.: New York, 2011; Vol. *1*, pp 313−327.
(72) Chipem, F. A. S.; Mishra, A.; Krishnamoorthy, G. Role of Hydrogen Bonding in Excited State Intramolecular Charge Transfer. *Phys. Chem. Chem. Phys.* **2012**, *14*, 8775−8790.
(73) Benesi, M. L.; Hildebrand, J. H. A Spectrophotometric Investigation of the Interaction of Iodine with Aromatic Hydrocarbons. *J. Am. Chem. Soc.* **1949**, *71*, 2703−2707.
(74) Singh, M. K.; Pal, H.; Koti, A. S. R.; Sapre, A. V. Photophysical Properties and Rotational Relaxation Dynamics of Neutral Red Bound to *β*-Cyclodextrin. *J. Phys. Chem. A* **2004**, *108*, 1465−1474.
(75) Voinov, M. A.; Kirilyuk, I. A.; Smirnov, A. I. Spin-Labeled pH-Sensitive Phospholipids for Interfacial pKa Determination: Synthesis and Characterization in Aqueous and Micellar Solutions. *J. Phys. Chem. B* **2009**, *113*, 3453−3460.
(76) Szejtli, J. *Cyclodextrins and Their Inclusion Complexes*; Akademiai Kiado: Budapest, 1982.
(77) Li, S.; Purdy, W. C. Cyciodextrins and Their Applications in Analytical Chemistry. *Chem. Rev.* **1992**, *92*, 1457−1490.

(78) Frisch, M. J.; Trucks, G. W.; Schlegel, H. B.; Scuseria, G. E.; Robb, M. A.; Cheeseman, J. R.; Montgomery, J. A., Jr.; Vreven, T.; Kudin, K. N.; Burant, J. C.; Millam, J. M.; Iyengar, S. S.; Tomasi, J.; Barone, V.; Mennucci, B.; Cossi, M.; Scalmani, G.; Rega, N.; Petersson, G. A.; Nakatsuji, H.; Hada, M.; Ehara, M.; Toyota, K.; Fukuda, R.; Hasegawa, J.; Ishida, M.; Nakajima, T.; Honda, Y.; Kitao, O.; Nakai, H.; Klene, M.; Li, X.; Knox, J. E.; Hratchian, H. P.; Cross, J. B.; Bakken, V.; Adamo, C.; Jaramillo, J.; Gomperts, R.; Stratmann, R. E.; Yazyev, O.; Austin, A. J.; Cammi, R.; Pomelli, C.; Ochterski, J. W.; Ayala, P. Y.; Morokuma, K.; Voth, G. A.; Salvador, P.; Dannenberg, J. J.; Zakrzewski, V. G.; Dapprich, S.; Daniels, A. D.; Strain, M. C.; Farkas, O.; Malick, D. K.; Rabuck, A. D.; Raghavachari, K.; Foresman, J. B.; Ortiz, J. V.; Cui, Q.; Baboul, A. G.; Clifford, S.; Cioslowski, J.; Stefanov, B. B.; Liu, G.; Liashenko, A.; Piskorz, P.; Komaromi, I.; Martin, R. L.; Fox, D. J.; Keith, T.; Al-Laham, M. A.; Peng, C. Y.; Nanayakkara, A.; Challacombe, M.; Gill, P. M. W.; Johnson, B.; Chen, W.; Wong, M. W.; Gonzalez, C.; Pople, J. A. *Gaussian 03*, revision E.01, Gaussian, Inc.: Wallingford, CT, 2004.

(79) Krishnamoorthy, G.; Dogra, S. K. Dual Fluorescence of 2-(4′-*N*,*N*-Dimethylaminophenyl)benzimidazole: Effect of β-Cyclodextrin and pH. *J. Photochem. Photobiol., A* **1999**, *123*, 109−119.

(80) El-Kemary, M.; Organero, J. A.; Santos, L.; Douhal, A. Effect of Cyclodextrin Nanocavity Confinement on the Photorelaxation of the Cardiotonic Drug Milrinone. *J. Phys. Chem. B* **2006**, *110*, 14128−14134.